Macromolecules

ARTICLE

pubs.acs.org/Macromolecules

Highly Conductive Polypyrrole/γ-Fe_2O_3 Nanospheres with Good Magnetic Properties Obtained through an Improved Chemical One-Step Method

Zhiming Zhang,[†] Qiong Li,[†] Liangmin Yu,[*,†] Zhijie Cui,[†] Lijuan Zhang,[*,‡] and Graham A. Bowmaker[‡]

[†]College of Chemistry and Chemical Engineering, Key Laboratory of Marine Chemistry, Theory and Technology, Ministry of Education, Ocean University of China, Qingdao, 266003, P. R. China

[‡]Polymer Electronics Research Centre, School of Chemical Sciences, University of Auckland, Private Bag 92019, Auckland, New Zealand

ABSTRACT: An improved chemical one-step method (ICOSM) was used to prepare highly conductive and magnetic polypyrrole/γ-Fe_2O_3 (PPy/γ-Fe_2O_3) nanospheres ~80 nm in diameter. In the reaction process involved, $FeCl_3$ acts as an oxidant for the polymerization of pyrrole and as a source of Fe^{III} for the formation of γ-Fe_2O_3, which also requires the initial presence of Fe^{II}, provided by the addition of $FeCl_2$. The method differs from the previous chemical one-step method (COSM) through the addition of *p*-toluenesulfonic acid (*p*-TSA) as the dopant after addition of the $FeCl_3$ solution was finished. The conductive and magnetic properties of PPy/γ-Fe_2O_3 nanospheres increased and reached maximum values simultaneously with increasing amounts of $FeCl_2$, contrary to the result observed in the previous COSM. The resulting electromagnetic PPy/γ-Fe_2O_3 nanospheres show maximum conductivity of 64.4 S/cm and saturation magnetization of 4.85 A m^2/kg. The *p*-TSA dopant plays a critical role in the formation of PPy/γ-Fe_2O_3 nanospheres.

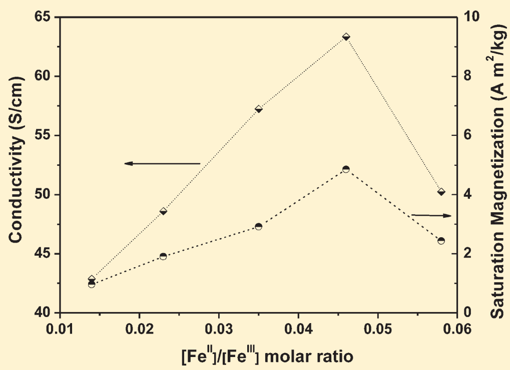

1. INTRODUCTION

Electromagnetically functionalized micro/nanostructures of conducting polymers are of special interest due to their potential applications in areas such as electromagnetic interference shielding,[1] microwave absorption,[2] nonlinear optics,[3] molecular electronics,[4] and biomedicine.[5] Previously, polyaniline (PANI) nanotubes containing Fe_3O_4 nanoparticles (~10 nm in diameter) have been prepared by an in-situ chemical oxidation polymerization (two-step method) in the presence of Fe_3O_4 nanoparticles.[6] The magnetic nanoparticles were prepared initially and were then incorporated in the oxidation polymerization of aniline to form the PANI/Fe_3O_4 nanotubes via a self-assembly process. We have also reported that coaxial PANI/γ-Fe_2O_3 nanofibers may be prepared by using γ-Fe_2O_3 nanoneedles as templates.[7] The above in-situ methods suffer from the limitation that the added magnetic particles rapidly aggregate, and so it is difficult to disperse them uniformly in the PANI matrix. More recently, we developed a very simple chemical one-step method (COSM) to prepare PANI/γ-Fe_2O_3 nanofibers.[8] The advantage of the COSM is that $FeCl_3$ acts as the oxidant for polymerization of aniline and as a source of Fe^{III} for the preparation of γ-Fe_2O_3 magnets, which results in a simultaneous preparation of the conducting polymer and the magnetic material, to form the electromagnetically functionalized composite nanofibers via a self-assembly process. By using this COSM, the magnetic γ-Fe_2O_3 nanoparticles can be integrated uniformly in the conducting polymer matrix. Thus, it is a simple and economical route to obtain electromagnetically functionalized composites in large quantity. However, all these electromagnetically functionalized PANI nanostructures show relatively low room-temperature conductivity (10^{-2}–10^{0} S/cm). In particular, good magnetic properties were usually accompanied by low electrical conductivity. Compared with PANI, polypyrrole (PPy) has a high conductivity, which encouraged researchers to synthesize electromagnetically functionalized PPy nanostructures using the above COSM. Thus, Xiao et al. have reported PPy/FeOOH nanospheres with a high conductivity of 16.1 S/cm by using the COSM.[9] However, the maximum saturation magnetization only is 0.11 A m^2/kg. Therefore, the preparation of a nanostructured conducting polymer composite with high electrical conductivity without compromising the magnetic properties is still a challenge.

In the present study, an improved chemical one-step method (ICOSM) was proposed to prepare uniform electromagnetic PPy/γ-Fe_2O_3 nanospheres with high conductivity and good magnetization. In our previously reported COSM,[8] no dopants were added into the polymerization solution. In order to get highly conductive composite nanostructures, *p*-TSA was added as dopant after the addition of $FeCl_3$ solution was finished. Through this ICOSM, the conductivity and magnetization can be

Received: March 21, 2011
Revised: May 17, 2011
Published: May 26, 2011

 © 2011 American Chemical Society

increased simultaneously by controlling the amounts of $FeCl_2$, which is added as the source of Fe^{II} that is required for the formation of γ-Fe_2O_3.[10] Of the resulting PPy/γ-Fe_2O_3 nanosphere products, the one that showed the maximum room temperature conductivity (64.4 S/cm) also had the highest saturation magnetization (M_s = 4.85 A m^2/kg).

2. EXPERIMENTAL PART

2.1. Chemicals. Pyrrole monomer (Py) was distilled under reduced pressure. Other reagents, such as ferric chloride ($FeCl_3 \cdot 6H_2O$), ferrous chloride ($FeCl_2 \cdot 4H_2O$), *p*-toluenesulfonic acid (*p*-TSA), and ammonium hydroxide (NH_4OH), were used as received without further purification.

2.2. Synthetic Method. A typical ICOSM procedure for the synthesis of electromagnetically functionalized PPy/γ-Fe_2O_3 composite nanospheres is as follows: Pyrrole monomer (0.133 mL, 2 mmol) was dissolved in aqueous ammonia solution (10 mL of 1.0 M) with ultrasonic stirring for 1 min to form white emulsion. Then a solution of $FeCl_2 \cdot 4H_2O$ (30 mg, 0.014 mmol) in water (5 mL) was added to the above emulsion, to yield a pale blue solution. To this was added a solution of $FeCl_3 \cdot 6H_2O$ (3.24 g, 12 mmol) in water (10 mL), dropwise at a rate of 1 mL/min, whereupon the solution immediately turned brown. During the addition of the $FeCl_3$ solution, the reaction solution was kept at 0−4 °C with stirring at the rate of 600 rpm. A quantity of *p*-TSA (0.34 g, 2 mmol) was added after addition of the $FeCl_3$ solution was finished. The reaction solution was stirred for 12 h. The resulting product was collected by centrifuging at 4000 rpm for 5 min. The powder was washed with distilled water, ethanol, and ether three times, respectively. Finally, the powder was dried under vacuum at room temperature for 24 h. The molar ratio of *p*-TSA to Py ([TSA]/[Py]) and the amounts of $FeCl_2 \cdot 4H_2O$ added (expressed as $[Fe^{II}]/[Fe^{III}]$, the ratio of added $[Fe^{II}]$ relative to initial $[Fe^{III}]$) were varied to investigate the effect of the preparation conditions on the morphology and on the electrical and magnetic properties of the PPy/γ-Fe_2O_3 composites.

2.3. Measurements. The morphology of the products was characterized by scanning electron microscopy (SEM, Hitachi-530 or FESEM, JSM-6700F). The room temperature conductivity was measured by a Keithley 196 SYSTEM DM digital multimeter and an ADVANTEST R6142 programmable dc voltage/current source using a standard four-probe method. The chemical structure was characterized by FTIR, XPS, and X-ray diffraction. The FTIR spectra of the composites in KBr pellets were recorded using an IFS-113 V instrument. XPS data were obtained with an ESCALab220i-XL electron spectrometer using Al Kα radiation under a base pressure of about 3×10^{-9} Torr. The binding energies were referenced to the C 1s line at 284.8 eV from adventitious carbon. X-ray diffraction was measured by a Micscience Model M18XHF diffractometer (MAC SCIENCE, Japan). Magnetization with an applied magnetic field (i.e., a hysteresis loop) at room temperature were carried out by using a vibrating sample magnetometer (VSM, Lakeshore 7307) with a maximum magnetic field of 795.77 kA/m.

3. RESULTS AND DISCUSSION

3.1. Electrical and Magnetic Properties of PPy/γ-Fe_2O_3 Nanospheres. In our previous COSM, the conductivity of PANI/γ-Fe_2O_3 nanofibers is only as high as 1.2 S/cm. Although Xiao et al.[9] reported that PPy/FeOOH nanospheres prepared by COSM can reach 16.1 S/cm, the saturation magnetization of 0.11 A m^2/kg is too low. In the preparation process of both PANI/γ-Fe_2O_3 nanofibers and PPy/FeOOH nanospheres, increasing the $FeCl_2$ amount results in more magnetic particles

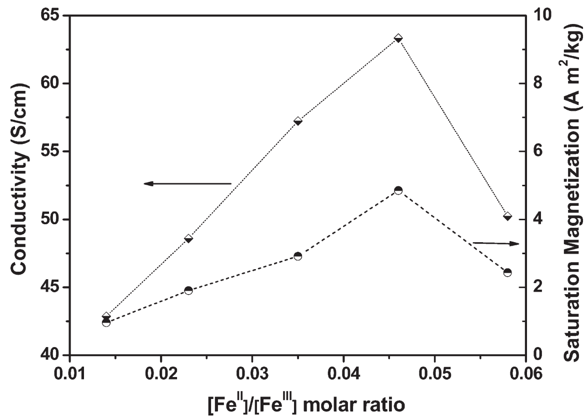

Figure 1. Effect of the $[Fe^{II}]/[Fe^{III}]$ ratios on the conductivity and saturation magnetization of PPy/γ-Fe_2O_3 composite nanospheres.

formed, which is favorable for good magnetic properties. However, increasing the $FeCl_2$ amount leads to decreased conductivity of the PANI/γ-Fe_2O_3 nanospheres. That is to say, it is hard to obtain the best electrical and magnetic properties at the same time using previous COSM. For our ICOSM, the enhancement caused by the $FeCl_2$ is favorable for both the electrical and magnetic properties when the $[Fe^{II}]/[Fe^{III}]$ ratio is lower than 0.046, which can be seen clearly from Figure 1. The conductivity of PPy/γ-Fe_2O_3 composite nanospheres increases from 42.9 to 64.4 S/cm with an increase in the $[Fe^{II}]/[Fe^{III}]$ ratio from 0.014 to 0.046. At the same time, the saturation magnetization of PPy/γ-Fe_2O_3 composite nanospheres also increases from 0.96 to 4.85 A m^2/kg when the $[Fe^{II}]/[Fe^{III}]$ ratio increases from 0.014 to 0.046. Moreover, the conductivity and the saturation magnetization of PPy/γ-Fe_2O_3 nanospheres simultaneously reached maxima of 64.4 S/cm and 4.85 A m^2/kg, respectively, when the $[Fe^{II}]/[Fe^{III}]$ ratio is 0.046. This positive increase of conductivity and magnetization with the increase of $FeCl_2$ amounts in this ICOSM is contrary to that observed in the previous COSM, in which the conductivity of PPy/γ-Fe_2O_3 composite nanospheres decreased with an increase in the amount of $FeCl_2$. All resulting PPy/γ-Fe_2O_3 composite nanosphere products in this ICOSM show high conductivity of 42.9−64.4 S/cm (as shown in Figure 1), which is greater by more than 3 orders magnitude compared with that of PANI/Fe_3O_4 nanotubes (~10^{-2} S/cm)[6] and by ~50 times compared with those of the PANI composite nanofibers (1.2 S/cm) and PPy/Fe_3O_4 nanoparticles (1.0 S/cm) by using the previous COSM.[8,11] Also, the conductivity of 42.9−64.4 S/cm for PPy/γ-Fe_2O_3 composite nanospheres obtained by using ICOSM is greater than that of PPy/γ-Fe_2O_3 composite (16.3 S/cm) prepared without *p*-TSA according to our previous COSM.[8] All these significant results can be attributed to the addition of *p*-TSA after addition of the $FeCl_3$ solution was finished. The reason that the conductivity of PPy/γ-Fe_2O_3 composite nanospheres increased with increasing the amount of $FeCl_2$ may be that more Cl^- will compete with TSA^- to dope into the PPy main chain with increasing amounts of $FeCl_2$ and lead to higher doping levels, which was confirmed by XPS data. As shown in Figure 2c, the binding energies of N 1s at 399.71 and 401.02 eV are observed, which are assigned to the undoped (−NH−) and doped (−N^+−) state of PPy, respectively.[12] The peak at 401.02 eV indicates that the PPy/γ-Fe_2O_3 composite nanospheres contain PPy in its doped state. The doping level can be calculated from the [−N^+−]/[−NH−] ratio. The doping

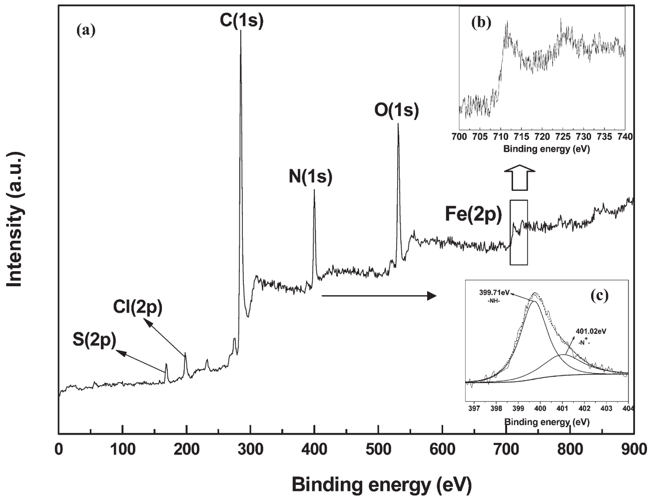

Figure 2. X-ray photoelectron spectra for PPy/γ-Fe_2O_3 composite nanospheres prepared at the [Fe^{II}]/[Fe^{III}] ratio of 0.046: (a) full survey spectrum; (b) expanded spectra of Fe 2p; (c) expanded spectra of N 1s.

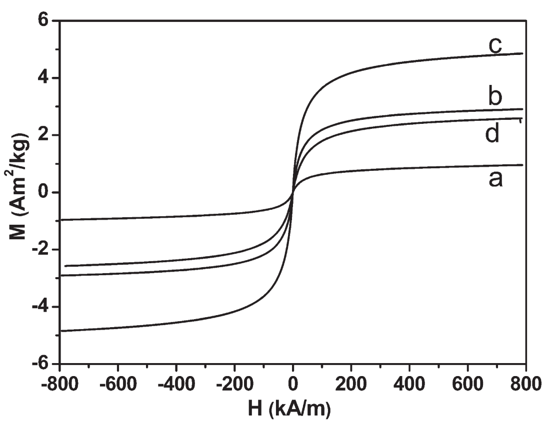

Figure 3. Dependence of magnetization on the applied magnetic field at room temperature for PPy/γ-Fe_2O_3 composite nanospheres synthesized at different [Fe^{II}]/[Fe^{III}] ratios: (a) 0.014, (b) 0.035, (c) 0.046, and (d) 0.058.

level of PPy/γ-Fe_2O_3 composite nanospheres increases from 28.07% to 37.24% when the [Fe^{II}]/[Fe^{III}] ratio increases from 0.014 to 0.046, which is consistent with the increase of conductivity.

In fact, the conductivity of PPy/γ-Fe_2O_3 composite nanopheres depends on two main factors: PPy and magnetic γ-Fe_2O_3 in the composite. Increasing the amount of $FeCl_2$ enhances the conductivity of PPy because the doping level increased from 28.07% to 37.24% when the [Fe^{II}]/[Fe^{III}] ratio increased from 0.014 to 0.046. At the same time, there is more magnetic γ-Fe_2O_3 produced with an increase in the amount of $FeCl_2$, which will result in a decrease in the conductivity of the PPy/γ-Fe_2O_3 composite. There are thus two competitive processes that contribute to the conductivity of the PPy/γ-Fe_2O_3 composite with increasing $FeCl_2$ amounts. In the earlier article,[8] the conductivity of the polyaniline/γ-Fe_2O_3 nanofibers decreased with increasing amounts of $FeCl_2$ because the decrease produced by γ-Fe_2O_3 exceeds the increase resulting from polyaniline. In our present ICOSM, it is obvious that the increase resulting from PPy exceeds the decrease produced by γ-Fe_2O_3.

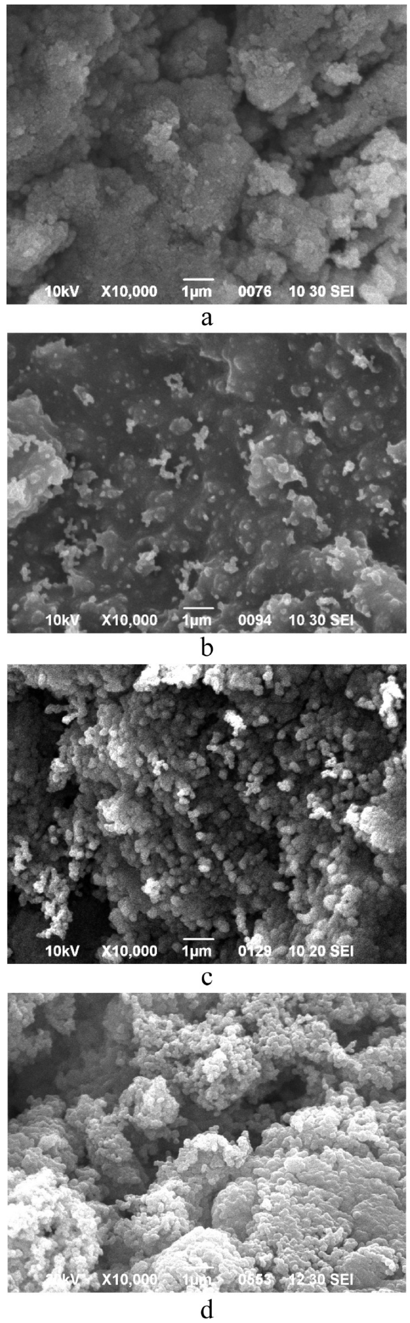

Figure 4. SEM images of PPy/γ-Fe_2O_3 composites prepared at different [TSA]/[Py] molar ratios: (a) 0, (b) 1, (c) 2, and (d) 3.

The increase in the electrical and magnetic properties with increasing amount of $FeCl_2$ is also different from the result reported by Zhang,[13] in which the increased amount of $FeCl_2$ resulted in higher magnetic properties but had no obvious effect on the conductivity of the PPy/Fe_3O_4 composite nanotubes. In Zhang's one-step method, pyrrole monomer, *p*-TSA, and $FeCl_3$ reacted for 2 h at first, and then $FeCl_2$ and ammonia were added to the solution. This method was indeed a two-step method because it contained two completely separate reaction process. The polymerization of pyrrole was finished in the first 2 h, and magnetic Fe_3O_4 was formed when the $FeCl_2$ and ammonia were added after the formation of PPy. So the addition of $FeCl_2$ has little influence on the conductivity of PPy/Fe_3O_4 composite nanotubes.

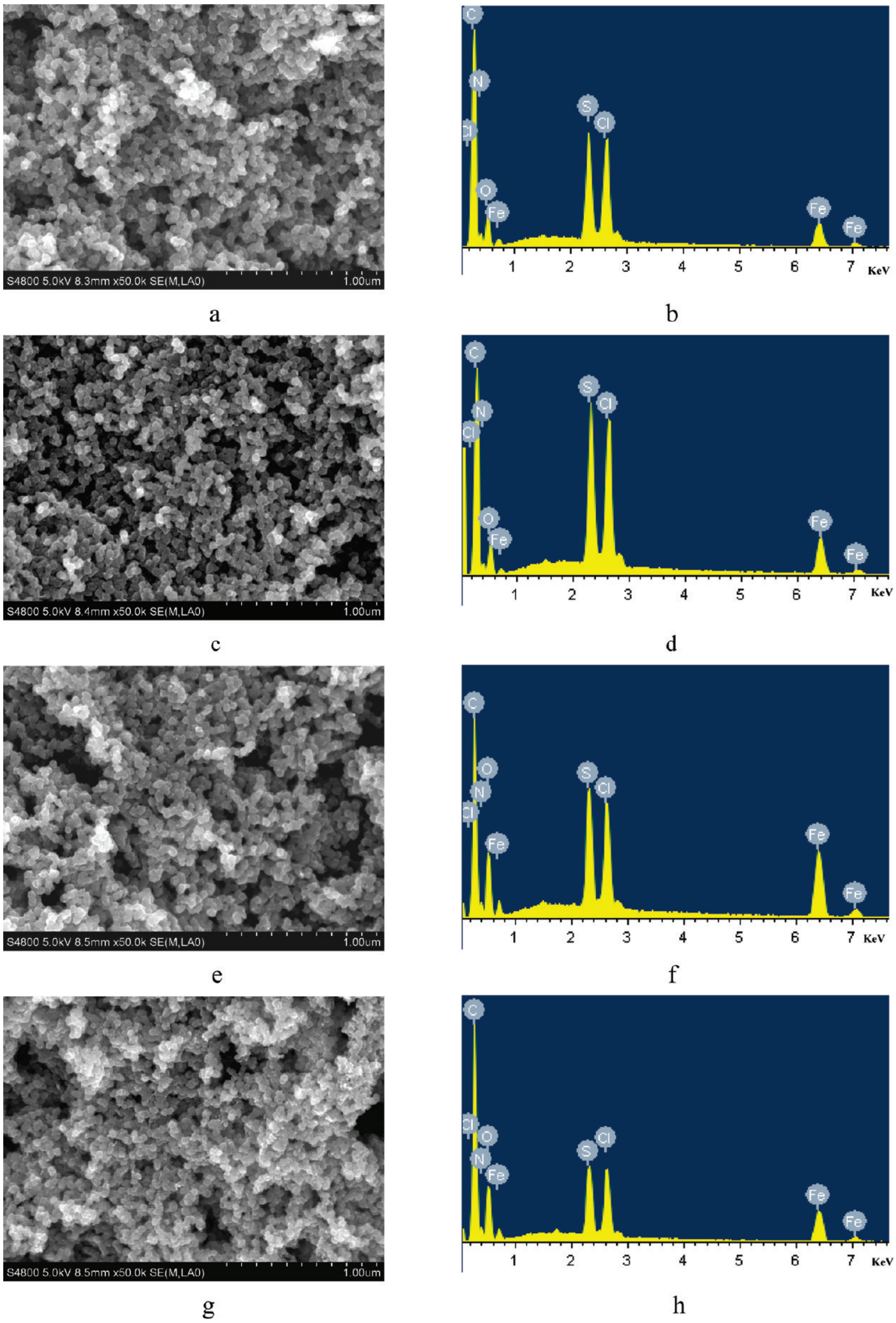

Figure 5. SEM images and EDAX spectra of PPy/γ-Fe_2O_3 composites prepared at different $[Fe^{II}]/[Fe^{III}]$ ratios: (a, b) 0.014, (c, d) 0.023, (e, f) 0.046, and (g, h) 0.058.

Figure 3 shows that the PPy/γ-Fe_2O_3 composite nanospheres exhibit superparamagnetic behavior (i.e., no hysteretic loop), and the saturation magnetization of the PPy/γ-Fe_2O_3 composite nanospheres increases from 0.96 to 4.85 A m^2/kg with an increase in the $[Fe^{II}]/[Fe^{III}]$ ratio from 0.014 to 0.046. This is because there are more γ-Fe_2O_3 magnetic particles formed when the amount of $FeCl_2$ is increased, which is similar to the results reported in the previous COSM.[8,9] However, the saturation magnetization decreases when the $[Fe^{II}]/[Fe^{III}]$ ratio is greater than 0.046.

3.2. Morphology. The uniform PPy/γ-Fe_2O_3 composite nanospheres were prepared successfully by using this ICOSM. In order to optimize the formation conditions for the PPy/γ-Fe_2O_3 composite nanospheres, the molar ratio of *p*-TSA to Py and the $[Fe^{II}]/[Fe^{III}]$ ratio in the reaction solution were investigated. It was found that [TSA]/[Py] molar ratio plays an important role in the formation of PPy/γ-Fe_2O_3 nanospheres. When [TSA]/[Py] molar ratio is 2, the uniform PPy/γ-Fe_2O_3 composite nanospheres were successfully prepared by ICOSM

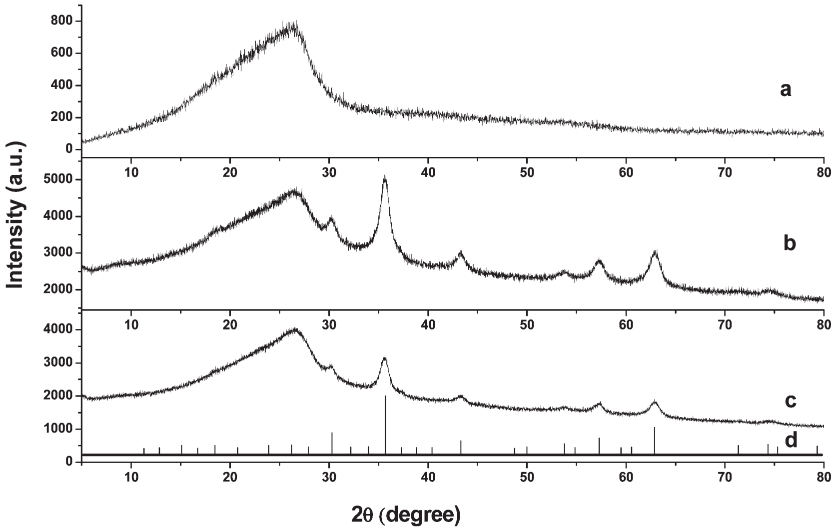

Figure 6. X-ray diffraction patterns of PPy, PPy/γ-Fe_2O_3 nanospheres, and γ-Fe_2O_3: (a) PPy doped with *p*-TSA; (b) PPy/γ-Fe_2O_3 nanospheres prepared with $[Fe^{II}]/[Fe^{III}]$ ratio of 0.046; (c) PPy/γ-Fe_2O_3 nanospheres prepared with $[Fe^{II}]/[Fe^{III}]$ ratio of 0.023; (d) standard γ-Fe_2O_3 (JCPDS No. 25-1402).

(Figure 4c). However, no uniform nanospheres can be observed (Figures 4b,d) when the [TSA]/[Py] molar ratio is lower than 1 or higher than 3. It needs to be noted that PPy/γ-Fe_2O_3 massive aggregates were obtained without any dopant added (Figure 4a). This result shows that *p*-TSA played a vital role in controlling the nanospheric morphology. Figure 5 shows the SEM images and EDAX spectra of the PPy/γ-Fe_2O_3 composites synthesized by using ICOSM at different $FeCl_2$ amounts when the [TSA]/[Py] molar ratio was kept at 2. It can be seen that the $FeCl_2$ amounts had no obvious effect on the spherical morphology, and uniform PPy/γ-Fe_2O_3 composite nanospheres can be obtained for all selected $[Fe^{II}]/[Fe^{III}]$ ratios (e.g., 0.014, 0.023, 0.046, and 0.058). Moreover, $FeCl_2$ amounts also had little influence on the diameter of the resulting PPy/γ-Fe_2O_3 nanospheres. The diameters of all PPy/γ-Fe_2O_3 nanospheres are ~80 nm. The EDAX spectra (Figures 5b,d,f, h) of PPy/γ-Fe_2O_3 composites show that C, N, Cl, S, and Fe, O elements were included in the nanospheres, which identified that the nanospheres are composed of PPy and iron oxide.

3.3. Formation Mechanism of PPy/γ-Fe_2O_3 Nanospheres. As reported in the Experimental Part, the aqueous $FeCl_2$ solution was added into the white emulsion of pyrrole and ammonia aqueous solution. Pyrrole micelles containing Fe^{2+} ions might be formed. According to previous reports,[14] the above-described micelles are regarded as the "soft templates" to form the electromagnetic composite nanospheres via a self-assembly process. The growth of the PPy nanostructures is allowed by an accretion[15] or elongation process.[16] It is obvious that the accretion process dominated in this ICOSM. In this process, $FeCl_3$ acts both as the oxidant for the polymerization of pyrrole to PPy and as a source of Fe^{III} for the formation of magnetic γ-Fe_2O_3. It is essential to add $FeCl_2$ and ammonia at the beginning for the formation of γ-Fe_2O_3.[10] The beginning pH value of the reaction solution is about 11−12 produced by ammonia, which is necessary and beneficial for the formation of Fe_3O_4 and then γ-Fe_2O_3. When the $FeCl_3$ was added, Fe^{3+} reacts with Fe^{2+} from the preadded $FeCl_2$ to form magnetic γ-Fe_2O_3 first in the base solution (pH = 11−12). With the addition of $FeCl_3$, pyrrole is also oxidized to PPy and Fe^{2+} is produced. Although Fe^{2+} can be produced with the oxidation polymerization of pyrrole, the Fe^{2+} produced is not available as a Fe^{2+} source to form Fe_3O_4 and then γ-Fe_2O_3. This is because the pH value of the reaction solution decreased promptly to <7 with the addition of $FeCl_3$, and the low pH value of the solution does not meet the strongly basic condition required for the formation of Fe_3O_4. Moreover, the extra *p*-TSA dopant was added in the reaction after the addition of the $FeCl_3$ aqueous solution. It was expected that the *p*-TSA would take part in the doping of PPy to improve the conductivity of PPy composites, and the presence of *p*-TSA in the product was shown by the XPS data. More Cl^- will compete with TSA^- to dope into the PPy main chain with increasing $FeCl_2$ content and lead to a higher doping level, which was also confirmed by the XPS data (Figure 2a).

3.4. Structural Characterization. Figure 6 shows the XRD patterns of PPy, PPy/γ-Fe_2O_3 nanospheres, and standard γ-Fe_2O_3. Only a broad peak centered at $2\theta = 25.1°$ is observed in the XRD pattern of PPy doped with *p*-TSA as shown in Figure 6a. Figures 6b,c show the XRD patterns of PPy/γ-Fe_2O_3 nanospheres obtained at the different $FeCl_2$ amounts. Apart from a broad peak attributed to PPy, the sharp peaks at $2\theta = 30.4°$, 35.7°, 43.4°, 53.8°, 57.3°, and 62.9° are also observed in the PPy/γ-Fe_2O_3 composite nanospheres, which correspond to the standard peaks of γ-Fe_2O_3 (JCPDS file No. 25-1402, Figure 6d).[17] This result indicates that γ-Fe_2O_3 exists in the PPy/γ-Fe_2O_3 composite nanospheres. The existence of γ-Fe_2O_3 was further supported by the XPS spectra, which is a powerful tool to differentiate between Fe_2O_3 and Fe_3O_4. As shown in Figure 2b, the photoelectron peaks at 711.1 and 724.4 eV, which are the characteristic doublets of Fe 2p3/2 and 2p1/2 core-level spectra of iron oxide, respectively, were observed for PPy/γ-Fe_2O_3 composite nanospheres. A relatively weak Fe 3p line at 55.9 eV was also detected. Both Fe 2p and 3p data matched very well with those of γ-Fe_2O_3 reported in the literature.[18] Moreover, these characteristic peaks of γ-Fe_2O_3 in the XRD pattern of PPy/γ-Fe_2O_3 nanospheres prepared with a $[Fe^{II}]/[Fe^{III}]$ ratio of 0.046 are stronger than those of γ-Fe_2O_3 in the XRD pattern of PPy/γ-Fe_2O_3 nanospheres at a $[Fe^{II}]/[Fe^{III}]$ ratio of 0.023, which shows that more magnetic γ-Fe_2O_3 formed in the

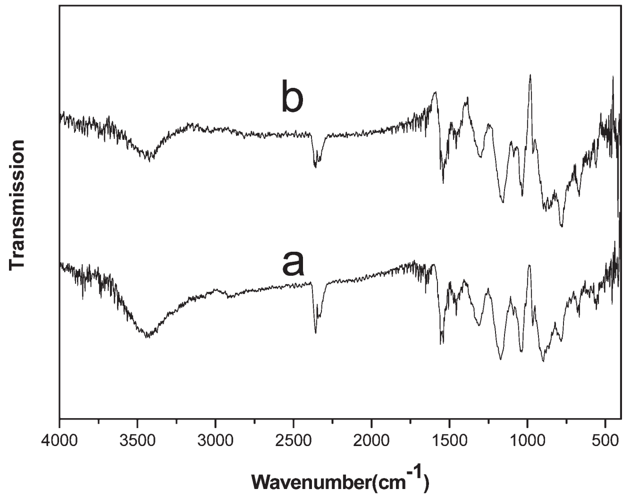

Figure 7. FTIR spectra for PPy/γ-Fe_2O_3 composite nanospheres prepared at different $[Fe^{II}]/[Fe^{III}]$ ratios: (a) 0.014 and (b) 0.046.

PPy/γ-Fe_2O_3 composite nanospheres when the $[Fe^{II}]/[Fe^{III}]$ ratio is 0.046. This result corresponds to the trend observed in their magnetic properties. Besides, all elements including C, N, S, Cl and Fe, O were found in the XPS spectra of the prepared composite nanospheres (Figure 2a), which further confirmed that the prepared nanospheres are composed of polypyrrole and γ-Fe_2O_3. Moreover, the presence of S and Cl in the XPS spectra indicated that both TSA^- and Cl^- are doped into the PPy main chain.

Figure 7 shows the FITR spectra of PPy/γ-Fe_2O_3 nanospheres obtained using different amounts of $FeCl_2$. The characteristic absorption bands at 1550, 1453, 1313, 1186, 1037, and 885 cm^{-1} for the PPy/γ-Fe_2O_3 composite nanospheres are similar to those of PPy/FeOOH and PPy/Fe_3O_4 synthesized via the previous COSM.[9,13] The peaks at 1550 and 1453 cm^{-1} are ascribed to the C=C and C−N stretching vibrations. The peaks at 1313 and 1186 cm^{-1} correspond to the C−H in-plane vibration. The peaks at 1037 and 885 cm^{-1} are attributed to the C−H in-plane bending and the ring deformation, respectively. These results indicate that the structure of the main PPy chain in the PPy/γ-Fe_2O_3 nanospheres prepared by the ICOSM is identical to those of the PPy/FeOOH and PPy/Fe_3O_4 nanostructures prepared by the previous COSM.[9,13]

4. CONCLUSION

PPy/γ-Fe_2O_3 composite nanospheres with high conductivity (42.9−64.4 S/cm), good saturation magnetization (∼4.85 A m^2/kg), and superparamagnetic properties (Hc = 0) were successfully prepared by an improved chemical one-step method (ICOSM). In this ICOSM, $FeCl_3$ acted both as the oxidant for the polymerization of pyrrole and as a source of Fe^{III} for the formation of γ-Fe_2O_3 magnets. Also, *p*-TSA as the dopant was added after the addition of $FeCl_3$, which played a very important role in enhancing the electrical properties and controlling the spherical morphology. Importantly, synchronous increasing and reaching the optimal electrical and magnetic properties of PPy/γ-Fe_2O_3 composite nanospheres can be realized by controlling the amounts of dopant and $FeCl_2$. Both the best saturation magnetization (4.85 A m^2/kg) and highest conductivity (64.4 S/cm) can be achieved for PPy/γ-Fe_2O_3 nanospheres in the same material when the $[Fe^{II}]/[Fe^{III}]$ ratio is 0.046. This ICOSM is thus a very simple and significant method for the preparation of highly conductive PPy/γ-Fe_2O_3 nanospheres with good magnetic properties, which opens a new way for the industrial application of electromagnetic conducting polymer nanostructures and will be a very useful to guide for the preparation of multifunctional nanostructured materials in a large quantity.

AUTHOR INFORMATION

Corresponding Author

*E-mail: yuyan@ouc.edu.cn (L.Y.); zhang.lijuan@hotmail.com (L.Z.).

ACKNOWLEDGMENT

The authors acknowledge Prof. Yunze long, Qingdao University, for his help and cooperation. This work was supported by National Natural Science Foundation of China (No. 50973098). The authors gratefully acknowledge the New Zealand Foundation for Science and Technology (No. UOAX0806).

REFERENCES

(1) Shen, P.; Huang, H.; Tseung, A. C. C. *J. Electrochem. Soc.* **1992**, *139*, 1840.

(2) (a) Miyauchi, S.; Aiko, H.; Sorimashi, Y.; Tsubata, I. *J. Appl. Polym. Sci.* **1989**, *37*, 289. (b) Yavuz, Ö.; Rama, M. K.; Aldissi, M.; Poddar, P.; Srikanth, H. *Synth. Met.* **2005**, *151*, 211.

(3) Peng, X.; Zhang, Y.; Yang, J.; Zhou, B.; Xiao, L.; Li, T. *J. Phys. Chem.* **1992**, *96*, 3412.

(4) (a) Gomez-Romero, P. *Adv. Mater.* **2001**, *13*, 163. (b) Suri, K.; Annapoorni, S.; Sarlar, A. K.; Tandon, R. P. *Sens. Actuators, B* **2002**, *81*, 277. (c) Geng, L. N.; Wang, S. R.; Zhao, Y. Q.; Peng, L.; Zhang, S. M.; Huang, W. P. *Mater. Chem. Phys.* **2006**, *99*, 15.

(5) Wuang, S. C.; Neoh, K. G.; Kang, E. T.; Pack, D. W.; Leckband, D. E. *J. Mater. Chem.* **2007**, *17*, 3354.

(6) Zhang, Z. M.; Wan, M. X. *Synth. Met.* **2003**, *132*, 205.

(7) Zhang, Z. M.; Wan, M. X.; Wei, Y. *Nanotechnology* **2005**, *16*, 2827.

(8) Zhang, Z. M.; Deng, J. Y.; Shen, J. Y.; Wan, M. X.; Chen, Z. J. *Macromol. Rapid Commun.* **2007**, *28*, 585.

(9) Xiao, H. M.; Zhang, W. D.; Fu, S. Y. *Compos. Sci. Technol.* **2010**, *70*, 909.

(10) (a) Khaleel, A. A. *Chem.—Eur. J.* **2004**, *10*, 925. (b) Kang, Y. S.; Risbud, S.; Rabolt, J. F.; Stroeve, P. *Chem. Mater.* **1996**, *8*, 2209.

(11) Xiao, H. M.; Zhang, W. D.; Wan, M. X.; Fu, S. Y. *J. Polym. Sci., Part A: Polym. Chem.* **2009**, *47*, 4646.

(12) Kang, E. T.; Neoh, K. G.; Ong, Y. T.; Tan, K. L.; Tan, B. T. G. *Macromolecules* **1991**, *24*, 2822.

(13) Zhang, W. D.; Xiao, H. M.; Zhu, L. P.; Fu, S. Y.; Wan, M. X. *J. Polym. Sci., Part A: Polym. Chem.* **2010**, *48*, 320.

(14) (a) Liu, J.; Wan, M. X. *J. Polym. Sci., Part A: Polym. Chem.* **2001**, *39*, 997. (b) Liu, J.; Wan, M. X. *J. Mater. Chem.* **2001**, *11*, 404. (c) Yang, Y. S.; Liu, J.; Wan, M. X. *Nanotechnology* **2002**, *13*, 771.

(15) Kim, B. J.; Oh, S. G.; Han, M. G.; Im, S. S. *Langmuir* **2000**, *16*, 5841.

(16) Harada, M.; Adachi, M. *Adv. Mater.* **2000**, *12*, 839.

(17) Search manual for powder diffraction data from the Joint Committee on Powder Diffraction Standards associateship at the National Bureau of Standards, 1st ed., The Committee in Swarthmore, PA, 1976.

(18) (a) Teng, X. W.; Black, D.; Watkins, N. J.; Gao, Y. L.; Yang, H. *Nano Lett.* **2003**, *3*, 261.(b) Cornell, R. M.; Schwertmann, U. In *The Iron Oxides: Structure, Properties, Reactions, Occurrence and Uses*; Wiley-VCH: Weinheim, Germany, 1996.